World Journal of Urology (2019) 37:2585–2595
https://doi.org/10.1007/s00345-019-02700-2

ORIGINAL ARTICLE

Pattern of metastatic deposit in recurrent prostate cancer: a whole-body MRI-based assessment of lesion distribution and effect of primary treatment

Vassiliki Pasoglou[1] · Nicolas Michoux[1] · Julien Van Damme[2] · Sandy Van Nieuwenhove[1] · Marin Halut[1] · Perrine Triqueneaux[1] · Bertrand Tombal[2] · Frédéric E. Lecouvet[1]

Received: 1 December 2018 / Accepted: 20 February 2019 / Published online: 2 March 2019

Abstract

Purpose It is generally accepted that when metastases develop in a patient with biochemical recurrence of prostate cancer (PCa), they follow a centrifuge pattern of seeding from the pelvis and that most patients enter the disease as oligometastatic. In this study, we used whole-body magnetic resonance imaging (WB-MRI) to assess the anatomical distribution of oligo- and polymetastatic disease and the impact of the initial treatment on this distribution in patients.

Materials and methods WB-MRI examinations of patients with a rising prostate-specific antigen (PSA) after radical treatment by surgery or/and radiotherapy were analyzed for disease recurrence. The patients were separated into three groups, based on the primary treatment: patients treated by radical prostatectomy without radiotherapy and with/without lymph node dissection (RP), patients treated only by radiotherapy or hormono-radiotherapy (RT) and patients treated with radical prostatectomy and adjuvant or salvage radiotherapy (RP + RT). Patients with ≤ 5 bone or/and node metastases were considered oligometastatic. Regional distributions of bone and lymph nodes metastases were reported using anatomical diagrams. Univariate and multivariable logistic regressions were performed to identify prognostic factors of relapse.

Results The primary treatment (RP, RT, RP + RT), Gleason score, PSA at relapse, time between first diagnosis and recurrence did not influence the metastatic status (oligo vs. polymetastatic). Oligometastatic patients showed different distribution of bone metastases compared to the polymetastatic ones and the distribution of the oligometastatic disease was not influenced by the primary treatment.

Conclusions In this WB-MRI-based study, there was no evidence that the primary treatment influenced the metastatic status of the patient or the distribution of the oligometastatic disease.

Keywords Whole-body magnetic resonance imaging · Whole-body MRI · Oligometastatic prostate cancer · Prostate cancer · Recurrence · Recurrent prostate cancer · Primary treatment · Metastasis distribution

Introduction

Prostate cancer (PCa) is a major health problem. Despite striking improvement in the treatment of localized disease, 30–40% of the patients treated by surgery and/or radiotherapy will develop prostate-specific antigen (PSA) recurrence [1]. Only one-third of these patients will develop metastases, in the lymph nodes or the skeleton. At this time, patients presenting one or a few metastases have better prognosis than those with widespread disease and may additionally benefit from salvage metastatic targeted therapies [2]. Yet, the factors that favor limited vs. extended metastatic spreading are not known. For instance, it is not known what the impact of localized treatment is.

✉ Vassiliki Pasoglou
vassiliki.pasoglou@uclouvain.be

[1] Department of Radiology, Centre Du Cancer and Institut de Recherche Expérimentale Et Clinique (IREC, IMAG), Cliniques Universitaires Saint-Luc, Université Catholique de Louvain (UCLouvain), Avenue Hippocrate 10, 1200 Brussels, Belgium

[2] Department of Urology, Cliniques Universitaires Saint-Luc, Avenue Hippocrate 10, 1200 Brussels, Belgium

The identification of the extent and location of metastases and the distinction between oligo- and polymetastatic diseases are critical to guide the choice between locoregional treatment and/or systemic therapy. That process has been widely impeded by the limited accuracy of the standard, guideline-approved, imaging modalities [3, 4]. Recent developments in radiology and in nuclear medicine offer more precise tools for early and accurate detection of metastatic disease. Whole-body magnetic resonance imaging (WB-MRI) and positron emission tomography (PET) with new specific radiotracers such as choline and prostate-specific membrane antigen (PSMA) ligand have the potential to alter the management of PCa patients with biochemical recurrence by detecting early onset of metastatic disease.

Most published studies focusing on the extent and the patterns of metastatic deposit in recurrent PCa have used PET-CT for disease detection [5–9]. In the present study, we report our observations with WB-MRI, which is a non-irradiating technique offering high soft tissue resolution for the detection of enlarged lymph nodes and the optimal imaging modality for studying the bone marrow. With the use of anatomic sequences combined with functional diffusion-weighted images (DWI), there is rarely need to administer contrast material to effectuate the staging of PCa patients.

The objective of this retrospective analysis was to study the anatomic distribution of metastases in PCa patients using WB-MRI and to assess the influence of the primary treatment on the metastatic status.

Materials and methods

Patient population

This is a retrospective analysis of 170 WB-MRI studies performed for the metastatic work-up of patients with biochemical recurrence after primary treatment. Patients were distributed into three groups:

Group 1: patients who underwent radical prostatectomy without radiotherapy and with/without lymph node dissection (RP).

Group 2: patients who were treated only by radiotherapy or hormone-radiotherapy-external beam therapy or brachytherapy (RT).

Group 3: patients who were treated with radical prostatectomy and adjuvant or salvage radiotherapy (RP + RT).

In all cases, clinical data were provided by the clinicians before the MRI exam. Table 1 summarizes patient characteristics.

Table 1 Patients' characteristics

Patient characteristics	
All patients	107
Status	
Oligometastatic	57
Polymetastatic	40
Local disease	10
Primary treatment	
RP (+ lymph node dissection)	38 (19)
RT (brachytherapy/+ lymph node irradiation)	34 (8/4)
RP + RT(+ lymph node dissection/+ lymph node irradiation)	35 (18/2)
Androgen deprivation therapy	
RP	12
RT	22
RP + RT	9
Age at PCA diagnosis (mean, IQR)	
Patients treated with RP	65 (56–73)
Patients treated with RT	64 (57–70)
Patients treated with RP + RT	64 (61–69)
Years of follow-up before relapse (mean, IQR)	
Patients treated with RP	6 (4–10)
Patients treated with RT	5 (3–9)
Patients treated with RP + RT	8 (5–11)
PSA at initial diagnosis (ng/ml) (median, IQR)	
Patients treated with RP	8 (5–11)
Patients treated with RT	17 (8–64)
Patients treated with RP + RT	8.3 (5–14)
No data available	15
Gleason score at initial diagnosis	
Patients treated with RP	7 (6–8)
Patients treated with RT	7 (6–8)
Patients treated with RP + RT	7 (6–7)
No data available	5
PSA at WB-MRI diagnosed relapse (ng/ml) (Median, IQR)	
Patients treated with RP	14 (3–82)
Patients treated with RT	10 (5–24)
Patients treated with RP + RT	14 (7–46)
No data available	7

WB-MRI protocol

Patients were imaged on 3.0-T MR units (Magnetom Verio; Siemens Healthineers, Erlangen, Germany, or Ingenia with Omega HP gradients, Philips Healthcare, Best, the Netherlands). The minimum WB-MRI protocol consisted of a whole-body coronal two-dimensional (head to toes or head to midthighs, thickness/gap: 4 mm/0.4 mm) or three-dimensional (head to midthighs, thickness/gap: 1.2/0) T1-weighted MRI pulse sequences and an axial

diffusion-weighted (DWI) MRI (head to midthighs, thickness/gap: 5 mm/0.5 mm). In addition, either a sagittal proton density fat suppression (PDFS) sequence of the whole spine (thickness/gap: 4 mm/0.4 mm) or a coronal STIR sequence of the whole body (thickness/gap: 4 mm/0) were performed.

Data analysis

The WB-MRI exams were analyzed independently and blindly by three readers with 5, 7, and 15 years of experience. For lymph node staging cervical, axillary, mediastinal, retroperitoneal, common external and internal iliac and inguinal nodes were defined as abnormal when the short-axis diameter was larger than 10 mm, or when there was loss of the normal oblong kidney bean shape or an irregular outline [10, 11]. We used a size threshold of 8 mm (short-axis diameter) for perivisceral abnormal lymph node (perivesical, perirectal, obturator, etc.) [10, 11]. Bone metastasis was defined as a lesion with low signal intensity T1, larger than 8 mm, and intermediate to high signal intensity on STIR or PDFS images, and high *b* values on diffusion-weighted images.

The following anatomic regions were defined for lesion detection: eight regions for bones (skull, humeri, thoracic cage including scapula, clavicules and sternum, cervical, dorsal and lumbar spine, pelvis, femurs) and eight regions for nodes [cervical, axillary, mediastinal, retroperitoneal (lumbo-aortic, retrocaval, laterocaval, etc.), common iliac, external iliac, internal iliac (locoregional) and inguinal].

Patients with ≤ 5 bone or/and node metastases were considered oligometastatic [12, 13].

Statistics

Descriptive statistics were performed by calculating medians and their interquartile range. Frequency distributions and proportions were summarized with percentages. Regional distributions of BM and LNM were reported using anatomical diagrams and bar graphs.

The Fisher–Freeman–Halton (FFH) exact test was used to assess the association between the patient's status and therapy at a significance level of $p < 0.05$ [14]. The proportion of oligometastatic patients within the patient groups were compared to each other using a one-sample proportion (1SP) test (based on the Newcombe-Wilson method for the mid-P approach and an expected proportion of 50%) [15]. Due to the three comparisons that were performed, the significance level of these tests was $p < 0.0167$.

PSA values at relapse and initial PSA values were compared in oligometastatic vs polymetastatic patients using the Mann–Whitney (*U*) test (as the normality of the data distribution was not verified according to the Shapiro–Wilk test). The initial Gleason values were compared between oligometastatic and polymetastatic patients using the Welch test (as the normality of the data distribution was verified, and as unequal variances were observed according to the *F* test). The significance level of the tests cited above was $p < 0.0167$.

The FFH exact test was used to assess the association between the organ (bone, lymph nodes, or bone + lymph nodes) that was found to be positive at relapse and the therapy followed by the patient. Oligometastatic and polymetastatic patients were grouped together for this analysis. The significance level was $p < 0.05$.

The FFH exact test was also performed to assess potential associations between the patient's status and the organ where the relapse was observed (BM, LNM or BM + LNM). The significance level was $p < 0.05$. The 1SP test was then applied to compare the proportions of BM, LNM, and BM + LNM patients to each other for both statuses. Due to the six comparisons that were performed, the significance level was $p < 0.0083$.

A Smirnov's (SMI) test on two-independent samples was done to assess whether the distribution of regions (positive to metastases) within a given organ is different in RP compared to RP + RT or in RT compared to RP + RT. This assessment was performed in oligometastatic patients then in polymetastatic patients. The significance level of this test was $p < 0.005$.

The frequency distribution of bone and lymph node regions (positive to metastases) was compared in oligometastatic and polymetastatic patients using the (SMI) test. The three therapies were pooled for this assessment. The significance level was $p < 0.025$.

Finally, a multivariable logistic regression analysis was performed to identify potential independent prognostic factors of the patient's status [16]. Factors tested were $\text{Gleason}^{\text{initial}}$, $\text{PSA}^{\text{initial}}$, $\text{PSA}^{\text{relapse}}$, time between first diagnosis and relapse, $\text{Age}^{\text{initial diagnosis}}$ and therapy. Each combination of one to six factors amongst six were tested using a backward selection procedure with a *p* value for a factor to enter the model set to 0.2, and a *p* value to leave the model set to 0.5. The significance level of the fit statistic was $p < 0.05$.

All calculations were performed with Statsdirect v3.1.14 (http://www.statsdirect.com/) and Matlab R2017a (MathWorks, Natick, MA, USA).

Results

Demographics

A total of 170 WB-MRI exams were analyzed. Sixty-three exams were excluded either because there was no

radiological proof of PCa local/nodal/bone recurrence or because of insufficient data (quality of exam, incomplete acquisition protocol, artifacts) (Fig. 1). Furthermore, ten exams were excluded because the recurrence was only local. Ninety-seven patients were considered metastatic. Fifty-seven patients were oligometastatic (≤ 5 lesions) and forty patients were polymetastatic (> 5 lesions) (Table 1).

Per-patient analysis

The histogram demonstrating the frequency distribution of oligometastatic and polymetastatic patients according to the primary treatment is shown in Fig. 2. Amongst the oligometastatic patients, twenty-one had been treated with RP (36.8%), fourteen with RT (24.6%) and twenty-two with RP + RT (38.6%); amongst the polymetastatic patients fourteen were treated with RP (35%), thirteen with RT (32.5%), and thirteen with RP + RT (32.5%).

No significant association was observed between the patient's status and therapy (FFH: $p = 0.0740$). The proportion of oligometastatic patients within each therapy group was not found to be significantly different from each other (1ST: $p^{\text{RP vs RT}} = 0.2430$, $p^{\text{RP vs RP+RT}} = 0.8804$, $p^{\text{RP + RT vs RT}} = 0.1877$).

No significant difference was found between oligometastatic and polymetastatic patients either in terms of initial PSA values, PSA values at relapse, or initial Gleason values (U: $p^{\text{initial PSA}} = 0.2091$, $p^{\text{relapse PSA}} = 0.3765$, $p^{\text{initial GLEASON}} = 0.1293$).

According to the ANOVA test, no organ (BM, LNM or BM + LNM) is found to yield a different initial Gleason score compared to at least another one, whatever the patient's status is ($p^{\text{oligometastatic}} = 0.9370$, $p^{\text{polymetastatic}} = 0.5110$).

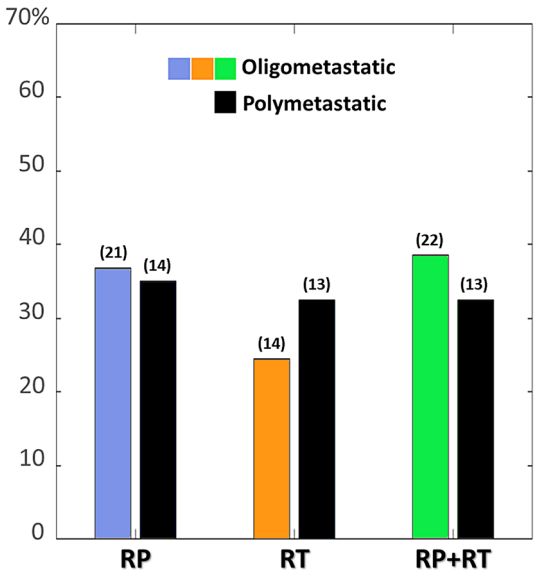

Fig. 2 Histogram demonstrating the frequency distribution of oligometastatic and polymetastatic patients according to the primary treatment. Numbers in brackets represent the number of patients per treatment

The frequency distribution of patients per organ (positive to metastases) and per therapy is shown in Fig. 3. When oligometastatic and polymetastatic patients were grouped together, no significant association was observed between the organ and the therapy (FFH: $p = 0.1533$).

The frequency distribution of oligometastatic and polymetastatic patients per organ (positive to metastases) is

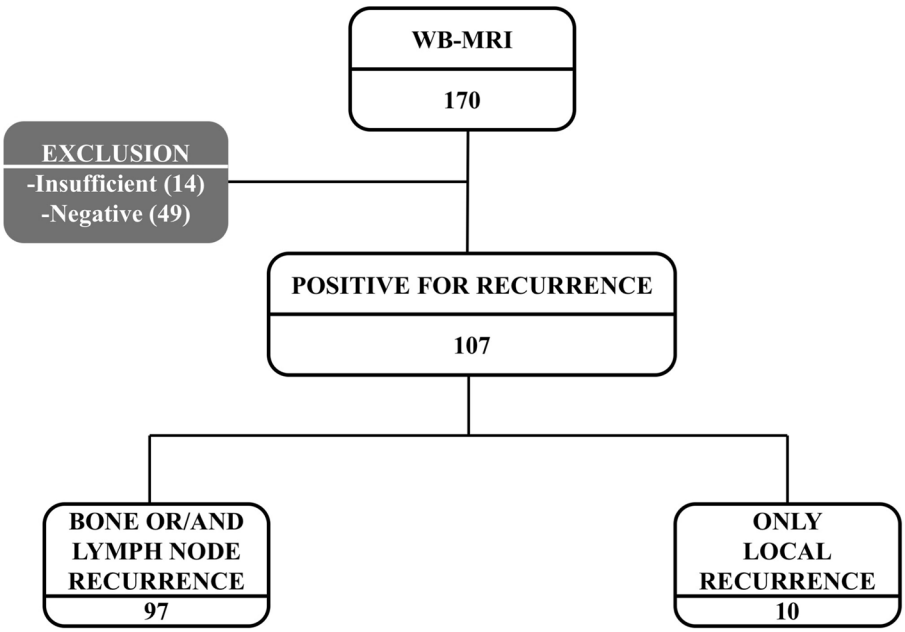

Fig. 1 Flow chart demonstrating the inclusion and exclusion algorithm

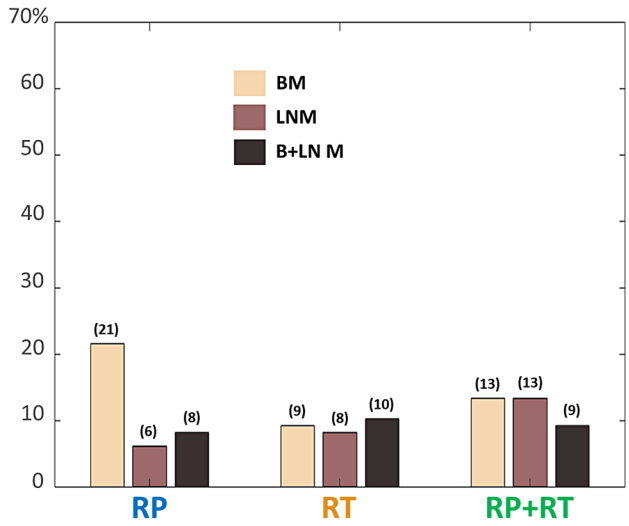

Fig. 3 Histogram demonstrating the distribution of patients per organ positive to metastases and per therapy. Numbers in brackets represent the number of patients

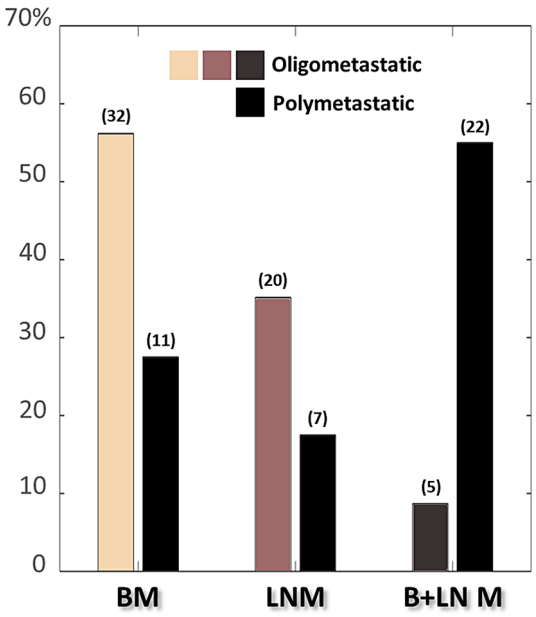

Fig. 4 Histogram demonstrating the frequency distribution of oligometastatic and polymetastatic patients per organ. Numbers in brackets represent the number of patients

shown on Fig. 4. In the group of oligometastatic patients 32/57 demonstrated BM disease, 20/57 LNM, and 5/57 both bone and lymph node recurrence. Amongst polymetastatic patients, 11/40 demonstrated BM, 7/40 LNM, and 22/40 both. A significant association was observed between the patient's status and the organ where the relapse is observed (FFH: $p < 0.0001$). In oligometastatic patients, statistically significant differences between

Table 2 Localization of BM in oligometastatic patients

Localisation	BM in oligometastatic patients (*n*: 37)
Skull	0 (0%)
Thoracic cage	5 (9.8%)
Humeri	1 (1.96)
Cervical spine	0 (0%)
Dorsal spine	7 (13.7%)
Lumbar spine	12 (23.5%)
Pelvis	23 (45.1%)
Femurs	3 (5.88%)

Table 3 Localization of LNM in oligometastatic patients

Localisation	LNM in oligometastatic patients (*n*: 25)
Cervical	1 (2.94%)
Axillary	0 (0%)
Mediastinal	2 (5.88%)
Retroperitoneal	9 (26.5%)
Common iliac	4 (11.8%)
External iliac	7 (20.6%)
Internal iliac/obturatory	9 (26.5%)

proportions of BM patients compared to B + LN M patients (1SP: $p^{\text{BM vs BM+LNM}} < 0.0001$) and in proportions of LNM patients compared to B + LN M patients (1SP: $p^{\text{LNM vs BM+LNM}} = 0.0025$) were demonstrated. However, no difference was observed between the proportions of BM and LNM patients (1SP: $p^{\text{BM vs LNM}} = 0.2717$). Amongst the polymetastatic patients, only 11/40 and 7/40 demonstrated recurrence within one single organ and the majority (22/40) relapsed both in the bone marrow and in the lymph nodes but with no statistically significant difference between the proportions of BM, LNM and B + LN M patients (1SP: $p^{\text{BM vs LNM}} = 0.8318$, $p^{\text{LNM vs BM+LNM}} = 0.0576$, $p^{\text{BM vs BM+LNM}} = 0.0351$).

Regarding the localization of BM in oligometastatic patients, 31/37 demonstrated at least one metastasis in the dorso-lumbar spine and pelvis (Table 2). This occurrence is significantly more frequent compared to that in other bone regions (1SP: $p^{\text{dorsolumbar+pelvis vs other bone}} < 0.0001$). When we analyzed the distribution of lymph node disease (Table 3), we observed that more than half of the patients presented at least one LNM outside the pelvis (15/25). This occurrence is not significantly different compared to that in other lymph nodes regions (1SP: $p^{\text{outside pelvis vs other lymph nodes}} = 0.4244$).

Per-region analysis

The frequency distribution of bone and lymph node regions (positive to metastases) per therapy in oligometastatic patients is shown in Fig. 5. There was no evidence that the distribution of positive bone regions was different according to therapy (SMI: $p^{\text{RP vs RP+RT}} = 0.9801$, $p^{\text{RT vs RP+RT}} = 0.6601$). We came to the same conclusion for the lymph nodes (SMI: $p^{\text{RP vs RP+RT}} > 0.9999$, $p^{\text{RT vs RP+RT}} > 0.9999$). A schematic overview of the distribution of bone and node disease per regions in oligometastatic patients is given in Fig. 6a.

The frequency distribution of bone and lymph node regions (positive to metastases) per therapy in polymetastatic patients is shown in Fig. 7. Within bone, there was strong evidence that the distribution of positive regions is different according to therapy (SMI: $p^{\text{RP vs RP+RT}} = 0.0002$, $p^{\text{RT vs RP+RT}} = 0.0002$). Within lymph nodes, there was no evidence for a difference according to therapy (SMI: $p^{\text{RP vs RP+RT}} = 0.9801$, $p^{\text{RT vs RP+RT}} = 0.9801$). In BM + LNM patients, there was strong evidence that the distribution of positive regions was different in RP compared to RP + RT (SMI: $p^{\text{RP vs RP+RT}} = 0.0007$), while there was no evidence of a difference in RT vs RP + RT (SMI: $p^{\text{RT vs RP+RT}} = 0.0933$). A schematic overview of the distribution of bone and node diseases per regions in polymetastatic patients is presented in Fig. 6b.

When comparing the frequency distributions on Figs. 5 and 7, we observed that within bone, when all therapies are pooled together, there is robust proof that the distribution of positive regions is different in oligometastatic patients compared to polymetastatic patients (SMI: $p^{\text{oligo vs poly}} = 0.0186$). Within lymph nodes, when all therapies were pooled together, there was no evidence of a difference

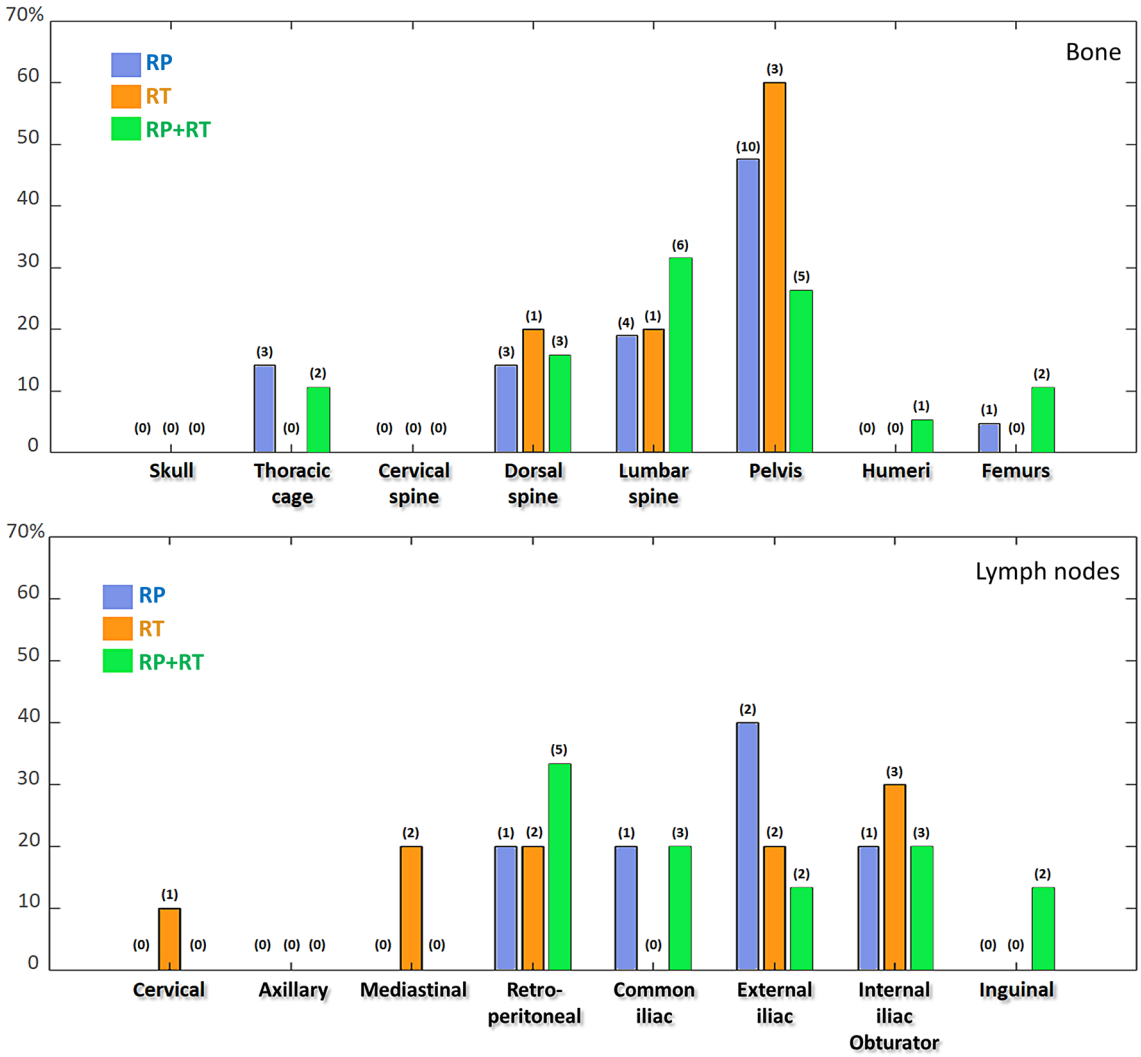

Fig. 5 Histogram demonstrating the frequency distribution of bone and lymph node regions positive for metastasis per therapy in oligometastatic patients. Numbers in brackets represent the number of positive regions observed within the studied cohort (RP, RT or RP + RT)

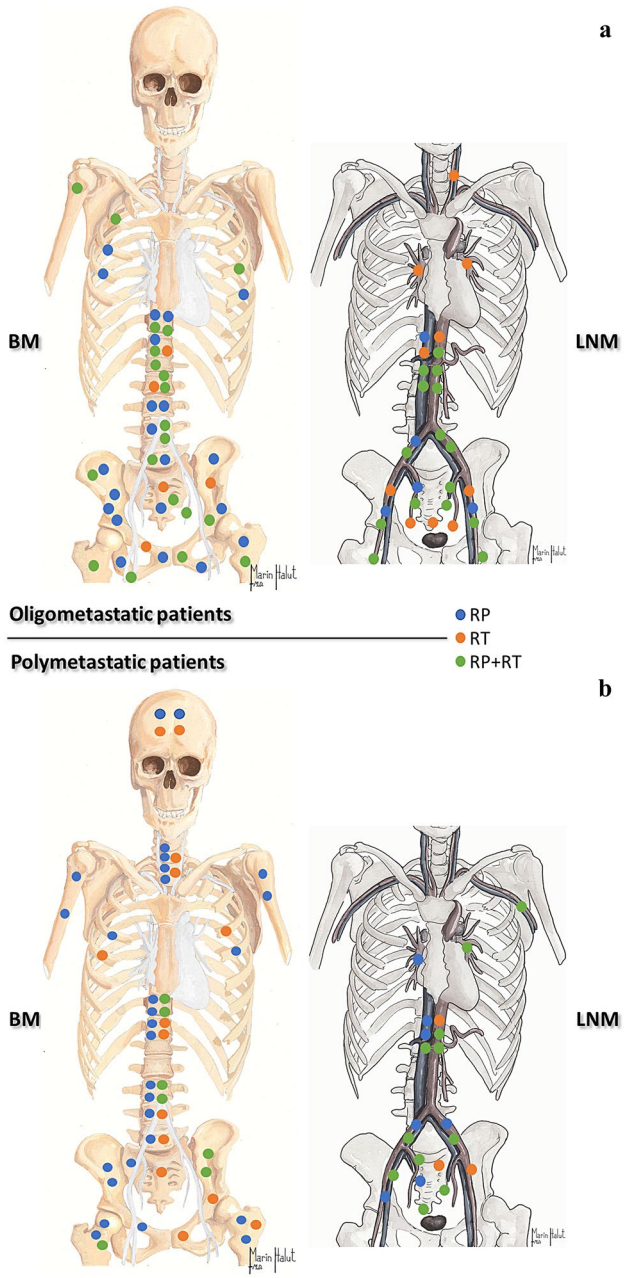

Fig. 6 Schematic overview of the distribution of bone and node disease per region in oligometastatic (**a**) and polymetastatic patients (**b**). Patients treated with radical prostatectomy (RP) are represented by blue colored cycles, with radiotherapy (RT) by orange colored cycles and with both radical prostatectomy and radiotherapy (RP+RT) by green colored cycles

in the distribution of positive regions between both groups (SMI: $p^{\text{oligo vs poly}} = 0.9801$).

Prognostic factors of the patient's status

Logistic regression models to predict the patient's status led to the following observations. A single model (univariate, based on factor $PSA^{relapse}$) yielded a significant fit statistic ($p = 0.0483$, with the outcome $z = 1/(1 + e^{-\text{logit}(z)})$ and $\text{logit}(z) = 0.2049 + 0.0016*PSA^{relapse}$). However, factor $PSA^{relapse}$ was not found to contribute significantly to the prediction at a significance level of 5% ($p = 0.1308$). It is worth noting that the biparametric model based on factors $PSA^{relapse}$ and time between first diagnosis and relapse, yielded an almost significant fit statistic ($p = 0.0670$), though here too, p values associated with both factors were not significant at 5%. Therefore, these models should be thoroughly investigated in a larger cohort of patients.

Discussion

Currently, little is known about the anatomic distribution of PCa recurrent disease. This study provides an initial insight of the topic using WB-MRI. Our data suggest that the primary treatment (RP, RT, RP + RT) does not affect the metastatic status of a patient (oligo- vs polymetastatic) or the proportions of BM and LNM. Additionally, neither of the Gleason score, PSA at relapse, time between first diagnosis and recurrence seem to influence the status of relapse and there is no correlation between Gleason score and site of relapse.

The concept of oligometastatic disease was first proposed by Hellmann and Weichselbaum in 1995 and until now there is no definitive consensus concerning the exact number of metastatic lesions for a patient to be considered as oligometastatic [2, 17]. Some definitions are based on both site and number of metastatic lesions. Most of the published studies imposed the limit of three or five metastases [12, 13, 17]; according to Singh et al. [18] patients with ≤ 5 metastatic sites have significantly better survival rates than patients with more than five metastases. Earlier, Solloway et al. [19] demonstrated that the survival of patients with ≤ 5 metastases differed significantly from those with > 20 metastases. This point was discussed during the 2017 Advanced Prostate Cancer Consensus Conference [20]. The panel did not reach consensus on what constitutes oligometastatic disease. From the subset of panelists who believed in the oligometastatic disease as a clinically meaningful entity, 14% voted that the patient must have ≤ 2 metastases to be considered oligometastatic, 66% ≤ 3 metastases, and 20% ≤ 5 metastases. Biologically speaking, however, the recent release of the radiotherapy arm of the Stampede trial shows an overall survival advantage only in patients with ≤ 4 non-visceral metastases [21].

Put in context, our finding that the initial treatment does not affect the metastatic status of a patient, may have several mechanistic explanations. Preliminary genomic data suggest that there are biological differences between widespread and oligometastatic disease in multiple cancers, including PCa

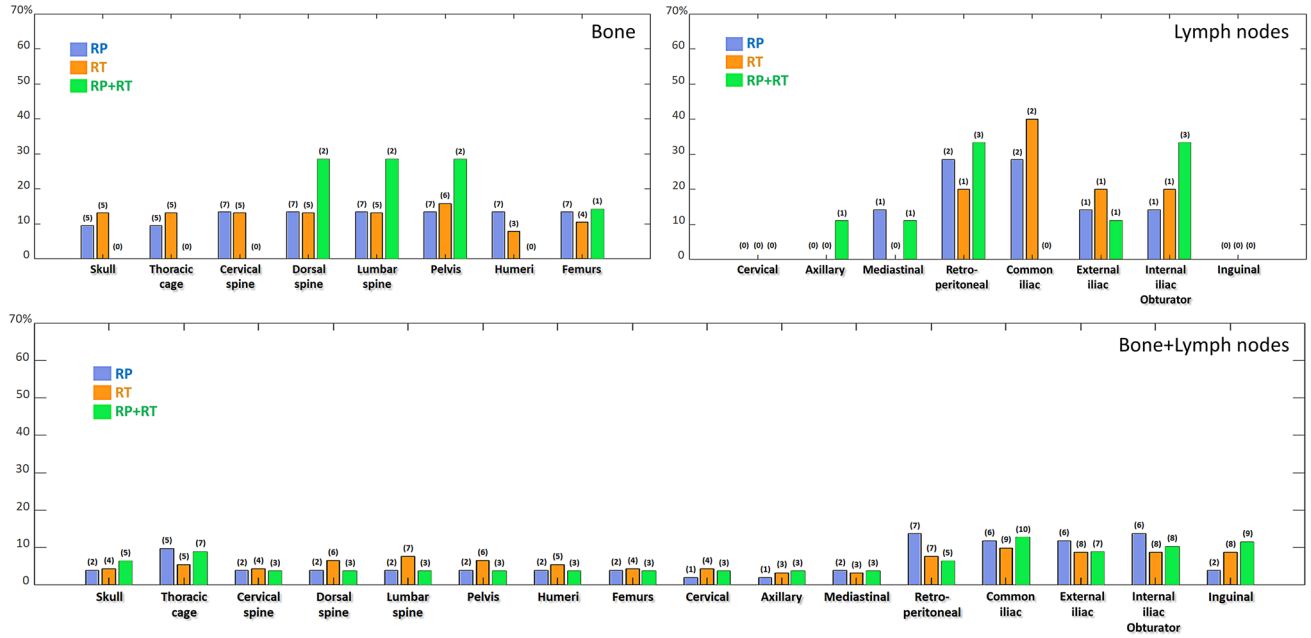

Fig. 7 Histogram demonstrating the frequency distribution of bone and lymph node regions positive for metastasis per therapy in polymetastatic patients. Numbers in brackets represent the number of positive regions observed within the studied cohort (RP, RT or RP + RT)

[22–24]. In this regard, genetic or biological factors may be more robust determinants of the metastatic status than the primary treatment. A more important challenge, which may explain the absence of effect of treatment, is whether the oligometastatic state is a stable situation or simply an earlier presentation of polymetastatic disease [20, 25]. Some oligometastatic lesions quickly progress to widespread metastases, others metastasize gradually, and others lack the capacity for widespread progression. Although the principles determining the dissemination of cancer cells are not completely clear, Gundem et al. [24] found that in metastatic PCa, metastasis-to-metastasis spread was common and that metastatic lesions can be seeded from other distant sites rather from the primary tumor. This observation is important, as targeting the existing metastases could be of paramount importance towards cure by preventing a widespread disease [12, 26, 27].

Ost et al. [26] demonstrated that in patients with oligometastatic recurrence, the androgen deprivation therapy-free survival was longer for patients with metastasis-directed therapy than for patients that underwent surveillance alone. Such therapies have been used in other neoplasias, such as non-small cell lung cancer [28], colon cancer [29] and renal cell carcinoma [30] with very good results.

The identification of oligometastatic PCa disease is usually based on validated imaging modalities such as bone scintigraphy (BS) and computed tomography (CT), and more recently on MRI and PET-CT. Even though there is compelling evidence supporting the low sensitivity and specificity of BS for the detection of bone metastasis and of thoraco-abdominal CT for the detection of lymph node metastasis, these techniques are routinely used in every day clinical practice in PCa patients [3, 4, 31]. It is clear, early and sensitive detection of oligometastatic disease is of crucial importance for the selection of the appropriate and optimal management and treatment of these patients. The latter entails the use of modern and novel imaging techniques namely PSMA PET-CT, PET-MRI, and WB-MRI [32–38].

Sobol et al. [8] in a mapping study identified the patterns of cancer relapse in patients with biochemical recurrence after prostatectomy, using ^{11}Choline PET-CT. The authors demonstrated that most forms of relapse show a combination of local or/and locoregional disease confined within the pelvis. In a recent study Parker et al. [39] studied the recurrence of PCa in patients with rising PSA post-radiotherapy and found that most relapses were localized within the pelvis soft tissue. In our study the patients with only local recurrence were excluded from analysis.

A recent study determined the patterns of progression after patients with recurrent oligometastatic disease received ^{68}Ga PSMA-ligand PET-CT-guided radiation therapy [40]. A ^{68}Ga PSMA-ligand PET-CT was performed in 76.6% of the patients with biochemical progressive disease after the treatment, confirming recurrent disease in 91.7% of them. Analysis of the irradiation treatment plan and the PET-CT concluded that 12.1% had a cumulative infield (in the prostatic fossa and irradiated lymph nodes) and 87.9% a cumulative outfield relapse rate. According to the authors

the number of positive pelvic lymph nodes decreased and there was a significant shift towards bone and distant lymph node disease.

Our results demonstrated that oligometastatic disease recurred more frequently only in the bone marrow or only in lymph nodes, rather than in both when the majority of the polymetastatic patients presented both bone and node relapses.

Gupta et al. [5] studied the distribution of PSMA avid disease both at the time of initial diagnosis and at disease recurrence. Patients treated only with radiotherapy demonstrated a lower incidence of metastatic lymph nodes in the mesorectal region but higher incidence of disease in the prostatic fossa. To appreciate the influence of adjuvant radiotherapy in patients with PCa recurrence, Rischke et al. [41] analyzed the site of new relapse after salvage lymph node dissection (SLND) alone, versus SLND with adjuvant radiotherapy (ART). In patients treated with SLND + ART, the proportion of patients with a new recurrent pelvic lymph node was significantly lower than in patients treated with SLND alone. The authors concluded that the addition of ART allows local control and improves relapse-free survival. Ost et al. [7] demonstrated that after stereotactic body radiotherapy (SBRT) for nodal oligometastasis, the new recurrence occurs in the lymph nodes and in an oligometastatic manner. In our study there was no evidence that primary treatment influenced the distribution of the metastatic disease in oligometastatic patients. In polymetastatic patients, primary treatment did influence the distribution of positive regions in bone. When a patient is treated with the combination of RP + RT, the relapse occurs mainly in dorso-lumbar spine and pelvis. When a patient is treated with RP or RT only, no preferential relapse site was observed. No differences were demonstrated regarding the locoregional lymph node relapse between treatments.

Lépinoy et al. [6] challenged the efficacy of the clinical-targeted volumes defined by the Radiation Therapy Oncology Group guidelines (CTV RTOG). The authors described the pattern of nodal relapse in patients with PCa with biochemical failure after prostate-only radiotherapy, using ^{18}F-Fluoro–Choline PET-CT and demonstrated that the number of positive lymph nodes confined within the CTV ROG area was significantly lower than the one outside this area. They concluded that if the upper field of intensity modulated radiation therapy (IMRT) was extended to L2–L3 it would cover 95% of the nodal stations at risk of an occult relapse, as 45.2% of the patients had relapsed outside the CTV RTOG. The same conclusions were supported by an earlier study investigating the geographical distribution of lymph node metastases with MR lymphography [42]. The authors demonstrated that 53% of the patients had at least one positive lymph node outside the CTV RTOG area. WB-MRI was used to study the metastatic spread of PCa in first diagnosis and during progression to castration-resistant PCa [9]. The authors showed that only 15% of newly diagnosed castration-naive patients and 25% of castration-resistant patients had disease restricted in the area of extended lymph node dissection. Furthermore, only 26% of the newly diagnosed patients and 30% of the castration-resistant patients had lymph node disease within the area targeted by external beam radiation therapy. In agreement with the aforementioned studies, our data demonstrated that 60% (15/25) of the oligometastatic patients with lymph node disease had a positive lymph node outside the pelvis.

In our study there was no significant evidence that factors such as PSA at relapse and time between the first diagnosis and recurrence influence the status of the patient at relapse (oligo- vs polymetastatic) but this should be investigated more thoroughly using a larger patient cohort.

Our study had several limitations. The small size of the studied cohort may have resulted in some differences between groups, to be rejected falsely. This is a retrospective analysis of WB-MRI exams effectuated in different machine systems. The treatment of the patients in every group was not the same, as some of them were treated with androgen deprivation therapy after the primary treatment and before WB-MRI detected metastatic relapse (Table 1). In the group of RP, some of the patients were treated by lymph node dissection and some not and for the RT patients some of the patients were treated with EBRT when others with brachytherapy and some received hormonotherapy, while others did not (Table 1).

Our data analysis was based on minimum sizes of 8 mm for focal bone lesions, 10 mm short axis for distant lymph nodes, and 8 mm short axis for regional lymph nodes. This use of size criteria to determine if a node is benign or malignant is a known pitfall in MRI and difficult to compare to metabolic studies.

Conclusions

At the time of salvage radiotherapy and direct curative therapy, it seems that no factors are predictive of oligo or polymetastatic recurrence. After primary treatment for PCa, most relapses occurred in the bone marrow or lymph nodes for the oligometastatic patients, while the majority of the polymetastatic patients presented both bone and node relapse. In this study, we found no evidence that the primary treatment (RP, RT, RP + RT) affected the metastatic status of a patient (oligo- vs polymetastatic). Furthermore, the primary treatment did not seem to affect the proportions of BM and LNM.

Finally, none of the parameters including age at first diagnosis, initial PSA value, or initial Gleason score seemed to predict if the patient will relapse as oligo- or polymetastatic.

Last, there was no significant difference in initial Gleason score between the different sites of relapse (BM, LNM or BM + LNM).

Author contributions VP, NM, JVD, SVN, BT, FEL: protocol/project development, data collection or management, data analysis, manuscript writing/editing. PT: data collection or management. MH: drawings

Compliance with ethical standards

Conflict of interest No conflicts of interest.

References

1. Roehl KA et al (2004) Cancer progression and survival rates following anatomical radical retropubic prostatectomy in 3478 consecutive patients: long-term results. J Urol 172(3):910–914
2. Hellman S, Weichselbaum RR (1995) Oligometastases. J Clin Oncol 13(1):8–10
3. Padhani AR et al (2017) Rationale for modernising imaging in advanced prostate cancer. Eur Urol Focus 3(2–3):223–239
4. Lecouvet FE et al (2012) Can whole-body magnetic resonance imaging with diffusion-weighted imaging replace Tc 99 m bone scanning and computed tomography for single-step detection of metastases in patients with high-risk prostate cancer? Eur Urol 62(1):68–75
5. Gupta SK et al (2017) Prostate-specific membrane antigen positron emission tomography-computed tomography for prostate cancer: distribution of disease and implications for radiation therapy planning. Int J Radiat Oncol Biol Phys 99(3):701–709
6. Lepinoy A et al (2014) Pattern of occult nodal relapse diagnosed with (18)F-fluoro–choline PET/CT in prostate cancer patients with biochemical failure after prostate-only radiotherapy. Radiother Oncol 111(1):120–125
7. Ost P et al (2016) Pattern of progression after stereotactic body radiotherapy for oligometastatic prostate cancer nodal recurrences. Clin Oncol R Coll Radiol 28(9):e115–e120
8. Sobol I et al (2017) Contemporary mapping of post-prostatectomy prostate cancer relapse with (11)C-Choline positron emission tomography and multiparametric magnetic resonance imaging. J Urol 197(1):129–134
9. Larbi A et al (2016) Whole body MRI (WB-MRI) assessment of metastatic spread in prostate cancer: therapeutic perspectives on targeted management of oligometastatic disease. Prostate 76(11):1024–1033
10. Eisenhauer EA et al (2009) New response evaluation criteria in solid tumours: revised RECIST guideline (version 1.1). Eur J Cancer 45(2):228–247
11. Koh DM, Hughes M, Husband JE (2006) Cross-sectional imaging of nodal metastases in the abdomen and pelvis. Abdom Imaging 31(6):632–643
12. Ahmed KA et al (2012) Stereotactic body radiation therapy in the treatment of oligometastatic prostate cancer. Front Oncol 2:215
13. Tabata K et al (2012) Radiotherapy for oligometastases and oligorecurrence of bone in prostate cancer. Pulm Med 2012:541656
14. Mehta CR, Patel NR (1983) A network algorithm for performing Fisher's exact test in r c contingency tables. J Am Stat Assoc 78:427–434
15. Newcombe RG (1998) Two-sided confidence intervals for the single proportion: comparison of seven methods. Stat Med 17(8):857–872
16. Pampel FC (2000) Logistic regression: a primer. Quantitative applications in the social sciences. Thousand oaks. Sage Publications, California
17. Tosoian JJ et al (2017) Oligometastatic prostate cancer: definitions, clinical outcomes, and treatment considerations. Nat Rev Urol 14(1):15–25
18. Singh D et al (2004) Is there a favorable subset of patients with prostate cancer who develop oligometastases? Int J Radiat Oncol Biol Phys 58(1):3–10
19. Solloway MJ et al (1998) Mice lacking Bmp6 function. Dev Genet 22(4):321–339
20. Gillessen S et al (2018) Management of patients with advanced prostate cancer: the report of the advanced prostate cancer consensus conference APCCC 2017. Eur Urol 73(2):178–211
21. Parker CC et al (2018) Radiotherapy to the primary tumour for newly diagnosed, metastatic prostate cancer (STAMPEDE): a randomised controlled phase 3 trial. Lancet 392:2353–2366
22. Tamoto E et al (2004) Gene-expression profile changes correlated with tumor progression and lymph node metastasis in esophageal cancer. Clin Cancer Res 10(11):3629–3638
23. Lussier YA et al (2011) MicroRNA expression characterizes oligometastasis(es). PLoS One 6(12):e28650
24. Gundem G et al (2015) The evolutionary history of lethal metastatic prostate cancer. Nature 520(7547):353–357
25. Murphy DG, Sweeney CJ, Tombal B (2017) "Gotta Catch 'em All", or do we? Pokemet approach to metastatic prostate cancer. Eur Urol 72(1):1–3
26. Ost P et al (2018) Surveillance or metastasis-directed therapy for oligometastatic prostate cancer recurrence: a prospective, randomized, multicenter phase II trial. J Clin Oncol 36(5):446–453
27. Muacevic A et al (2013) Safety and feasibility of image-guided robotic radiosurgery for patients with limited bone metastases of prostate cancer. Urol Oncol 31(4):455–460
28. Richard PJ, Rengan R (2016) Oligometastatic non-small-cell lung cancer: current treatment strategies. Lung Cancer (Auckl) 7:129–140
29. Simmonds PC et al (2006) Surgical resection of hepatic metastases from colorectal cancer: a systematic review of published studies. Br J Cancer 94(7):982–999
30. Graves A et al (2013) Metastatic renal cell carcinoma: update on epidemiology, genetics, and therapeutic modalities. Immunotargets Ther 2:73–90
31. Lecouvet FE et al (2007) Magnetic resonance imaging of the axial skeleton for detecting bone metastases in patients with high-risk prostate cancer: diagnostic and cost-effectiveness and comparison with current detection strategies. J Clin Oncol 25(22):3281–3287
32. Hirmas N, Al-Ibraheem A, Herrmann K, Alsharif A, Muhsin H, Khader J, Al-Daghmin A, Salah S (2018) [^{68}Ga]PSMA PET/CT improves initial staging and management plan of patients with high-risk prostate cancer. Mol Imaging Biol. https://doi.org/10.1007/s11307-018-1278-8
33. Padhani AR et al (2017) METastasis reporting and data system for prostate cancer: practical guidelines for acquisition, interpretation, and reporting of whole-body magnetic resonance imaging-based evaluations of multiorgan involvement in advanced prostate cancer. Eur Urol 71(1):81–92
34. Park SY et al (2018) Gallium 68 PSMA-11 PET/MR imaging in patients with intermediate- or high-risk prostate cancer. Radiology 288(2):495–505
35. Dyrberg E et al (2018) (68)Ga-PSMA-PET/CT in comparison with (18)F-fluoride-PET/CT and whole-body MRI for the detection of bone metastases in patients with prostate cancer: a prospective diagnostic accuracy study. Eur Radiol 29:1221–1230
36. Pasoglou V et al (2014) One-step TNM staging of high-risk prostate cancer using magnetic resonance imaging (MRI): toward

an upfront simplified "all-in-one" imaging approach? Prostate 74(5):469–477
37. Pasoglou V et al (2015) Whole-body 3D T1-weighted MR imaging in patients with prostate cancer: feasibility and evaluation in screening for metastatic disease. Radiology 275(1):155–166
38. Lecouvet FE et al (2018) Use of modern imaging methods to facilitate trials of metastasis-directed therapy for oligometastatic disease in prostate cancer: a consensus recommendation from the EORTC imaging group. Lancet Oncol 19(10):e534–e545
39. Parker WP et al (2017) Identification of site-specific recurrence following primary radiation therapy for prostate cancer using C-11 choline positron emission tomography/computed tomography: a nomogram for predicting extrapelvic disease. Eur Urol 71(3):340–348
40. Soldatov A et al (2019) Patterns of progression after (68) Ga-PSMA-ligand PET/CT-guided radiation therapy for recurrent prostate cancer. Int J Radiat Oncol Biol Phys 103(1):95–104
41. Rischke HC et al (2015) Adjuvant radiotherapy after salvage lymph node dissection because of nodal relapse of prostate cancer versus salvage lymph node dissection only. Strahlenther Onkol 191(4):310–320
42. Meijer HJ et al (2013) Geographical distribution of lymph node metastases on MR lymphography in prostate cancer patients. Radiother Oncol 106(1):59–63